Quench Instabilities of a Strongly Interacting Quantum Gas in an Optical Cavity

Filip Marijanović,[1,*,†] Sambuddha Chattopadhyay,[1,2,*] Luka Skolc,[1] Timo Zwettler,[3] Catalin-Mihai Halati,[4] Simon B. Jäger,[5] Thierry Giamarchi,[4] Jean-Philippe Brantut,[3] and Eugene Demler[1]

[1]*Institute for Theoretical Physics, ETH Zürich, CH-8093 Zürich, Switzerland*

[2]*Lyman Laboratory, Department of Physics, Harvard University, Cambridge, Massachusetts 02138, USA*

[3]*Institute of Physics, Ecole Polytechnique Fédérale de Lausanne, Lausanne, Switzerland*

[4]*Department of Quantum Matter Physics, University of Geneva, Quai Ernest-Ansermet 24, 1211 Geneva, Switzerland*

[5]*Physics Department and Research Center OPTIMAS, University of Kaiserslautern-Landau, D-67663, Kaiserslautern, Germany*

(Received 1 August 2024; revised 20 March 2026; accepted 9 April 2026; published 14 May 2026)

Recent quench experiments on ultracold atoms in optical cavities provide a clean platform for studying how long-range interactions in atomic media structure their nonequilibrium dynamics. Motivated by these experiments, we provide a theoretical analysis of the quench instabilities that lead to the formation of superradiance as the hybrid system is driven across the self-organization transition. Working with both ultracold bosonic and fermionic gases, we compute the rate at which order forms and quantify the fluctuations of the prequench state that seed the instability. Our results quantitatively match existing experiments on free fermions and make predictions for quench experiments involving interacting Bose and Fermi gases. Our Letter suggests that the nonlocal nature of the photon-mediated interactions generates ordering dynamics that are qualitatively different than those observed in short-range interacting systems.

DOI: 10.1103/w2vx-t1mr

Introduction—How fast does order grow in a many-body system as it is quenched across a quantum phase transition? The answer to this question—demanding replies from contexts as varied as cosmology [1], soft matter [2], solid-state physics [3], and cold atoms [4–7]—is typically constrained by *locality*. As a concrete illustration of locality-constrained pattern formation, experiments on ultracold Bose gases have observed the emergence of spatial structure following quenches, including spin-domain formation in spinor condensates [8,9], modulational instabilities [10,11], and Kibble-Zurek defect formation [12,13]. In all these systems, the growth of order is constrained by locality: correlations propagate with a finite velocity set by microscopic energy scales, and patterns emerge from the amplification and coarsening of local fluctuations. What complications arise, then, when we ask the question in a system with nonlocal interactions?

Recent experiments [14,15] investigating the quench dynamics of ultracold quantum gases in an optical cavity present an ideal laboratory for such questions [16–22]. In these experiments, strong cavity-mediated all-to-all interactions are engineered by loading quantum degenerate atoms into a cavity and driving them with a transverse pump [23–29]. Under sufficiently strong driving, the initially homogeneous gas self-organizes to develop density wave order, which concomitantly supports the superradiant buildup of intracavity photons [27,30–33]. In the quench experiments [14,15], the transverse pump power is rapidly increased, bringing the system from the normal phase to the ordered phase. Given the (weakly) dissipative nature of the cavity, photons leak out of the cavity in the superradiant phase [14,15]. Remarkably, the leaked photons provide a high-resolution *in vivo* probe, allowing experiments to monitor the dynamics of superradiant self-organization.

In this Letter, we calculate how fast the intertwined density and superradiant orders develop in the system after a quench, quantifying both the initial fluctuations that seed the instability as well as the rate of the order's exponential growth. Leveraging linear response theory, we make direct contact with experiments involving a wide class of atomic media, matching growth rate measurements for dissipative free fermions coupled to an optical cavity and predicting rates for cavity quench experiments performed on interacting bosons and fermions. We conclude by extrapolating our theoretical results to regimes beyond current experiments, commenting on how nonlocal interactions alter the dynamics of ordering in many-body systems.

Model—We consider atoms in the lower energy internal state of a two-component, quantum degenerate gas dispersively coupled to an optical cavity with wave vector $\mathbf{k}_c$, which is transversely driven by a retroreflected laser with wave vector $\mathbf{k}_p$ [14,15,28,29] (see Fig. 1). In the rotating frame of the pump, the effective Hamiltonian is given by [29]

$$H = H_{\mathrm{at}} + \frac{\Delta_c}{2}(x^2 + p^2) + H_{\mathrm{int}}, \tag{1}$$

*These authors contributed equally to this work.

†Contact author: fmarijanovic@ethz.ch

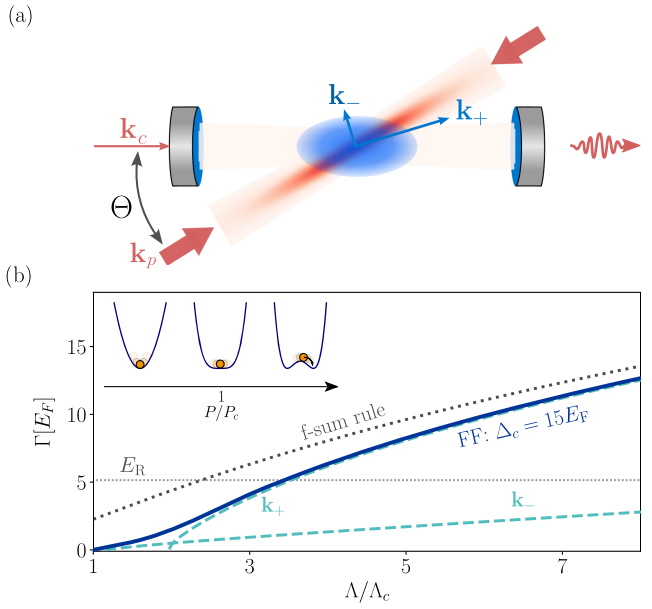

FIG. 1. Instability rate. (a) Experimental schematic of pump incoming at an angle Θ with respect to the cavity. For powers above the phase transition, the system is superradiant, and the atomic density orders at two wave vectors $\mathbf{k}_{\pm}$, given by cavity and pump wave vectors $\mathbf{k}_{c/p}$, respectively. (b) The instability growth rate Γ for 3D free fermions (FF) in units of the Fermi energy E_F as a function of the reduced quenched photon-fermion coupling strength Λ/Λ_c for pump-cavity detunings $\Delta_c = 15E_F$. Dashed lines show contributions from the two ordering wave vectors, $|\mathbf{k}_+| = 2.24k_F$ and $|\mathbf{k}_-| = 0.36k_F$. For deep quenches, the rate approaches a universal value, given by the f-sum rule (dotted). The horizontal line indicates recoil energy, corresponding to the speed limit of short-range interactions. The inset shows the Ginzburg-Landau free energy across the phase transition.

where H_{at} is a generic atomic (bosonic or fermionic) Hamiltonian, Δ_c is the *effective* photon detuning (accounting for the collective dispersive shift from the atoms), and x, p are photon quadratures. H_{int} is the fermion-cavity coupling, given by

$$H_{\text{int}} = \sqrt{N}\eta(t)x\sum_{Q}(\rho_Q + \rho_{-Q}), \tag{2}$$

where the atomic density operator at wave vector $Q \in \{\mathbf{k}_{\pm} = \mathbf{k}_c \pm \mathbf{k}_p\}$ is written as $\rho_Q = (1/\sqrt{N})$ $\sum_{p,\sigma} c^{\dagger}_{p+Q,\sigma}c_{p,\sigma}$, and $c^{\dagger}_{p\sigma}(c_{p\sigma})$ are atomic creation (annihilation) operators that create (annihilate) an atom of momentum p (and spin σ for fermions). While more involved Hamiltonians can arise in realistic experimental settings—accounting for, e.g., multiple cavity polarizations [29,33]—Eq. (2) provides a minimal model for superradiant physics in cavity-quantum gas experiments [34]. The coupling strength $\eta(t)$ can be tuned by modulating the power of the transverse driving field. We also temporarily neglect cavity dissipation. In the absence of dissipation, the steady state of the system is superradiant above $\eta_c = \frac{1}{2}\{\Delta_c/[\sum_Q \chi(Q)N]\}^{\frac{1}{2}}$ [29,31], where $\chi(Q) \equiv \chi(Q, \omega = 0)$ is the static atomic density susceptibility at wave vector Q.

Instability rate—Having summarized the steady-state phases of our system, we now consider a quench of the light-matter interaction $\eta(t)$ from 0 to $\Lambda \geq \eta_C$ at $t = 0$. After a brief transient regime, density order rapidly forms, growing as $\rho_Q(t) \simeq \rho_{Q,0}e^{\Gamma t}$, while cavity photons simultaneously proliferate exponentially, as $n(t) \simeq n_0 e^{2\Gamma t}$ in the unstable regime [35]. We calculate the growth rate Γ by studying the dynamics of the unstable, polaritonic collective mode within linear response, as is appropriate while the exponentially growing order built up in the system is small in comparison to its maximum value set by nonlinearities. We begin by writing down the Heisenberg equations of motion for the photonic quadratures in frequency space: $i\omega x = \Delta_c p; i\omega p = -\Delta_c x - \sqrt{N}\eta(t)\sum_Q \rho_Q$. Next, we recognize that H_{int} has the form of the *gedanken* probe field used to derive the fermionic density susceptibility within linear response. Leveraging this association, we write $\rho_Q = \sqrt{N}\eta(t)\chi(Q,\omega)x$, where $\chi(Q,\omega)$ is the (dynamical) atomic density susceptibility at frequency ω and wave vector Q. We model the quench by taking $\eta(t = 0^+) = \Lambda$ and $\chi(Q,\omega)$ of a possibly interacting ultracold atomic gas, initially uncoupled to cavity photons. The resulting frequency of the polaritonic mode is

$$\omega^2 = \Delta_c^2 - 4\Lambda^2 N\Delta_c \sum_Q \chi(Q,\omega). \tag{3}$$

Our self-consistency equation admits purely unstable, imaginary solutions $\omega = \pm i\Gamma$ beyond a critical coupling Λ_c—see the Supplemental Material [36] for details. Using the spectral representation, we can recast the self-consistent equation for Γ as

$$1 + \Gamma^2\Delta_c^{-2} = \frac{4\Lambda^2 N}{\Delta_c}\sum_Q \int_{-\infty}^{\infty}\frac{d\omega}{\pi}\frac{\omega\Im\chi(Q,\omega)}{\omega^2 + \Gamma^2}. \tag{4}$$

Our analysis is completely general within linear response theory, allowing for *quantitative* comparison with experiments involving myriad atomic media (e.g., fermions or bosons, free or interacting, homogeneous or harmonically trapped, zero or finite temperature). We emphasize that all relevant microscopic information enters via the density response function $\chi(Q,\omega)$.

Asymptotic insight into Eq. (4) can be gained by considering the sum rules imposed on $\text{Im}\chi(Q,\omega)$. The low-frequency behavior of $\text{Im}\chi(Q,\omega)$ is constrained by a generalized "finite-Q" compressibility rule arising from the Kramers-Kronig relations on $\text{Im}\chi(Q,\omega)$: $\int d\omega\omega^{-1}\,\text{Im}\chi(Q,\omega) = \pi\chi(Q)$. This compressibility sum rule can be used to find the critical quench strength $\Lambda_c = \frac{1}{2}\{\Delta_c/[\sum_Q \chi(Q)N]\}^{\frac{1}{2}} = \eta_c$, as expected from the

Ginzburg-Landau free energy picture (see Fig. 1). The high-frequency behavior of $\mathrm{Im}\chi(Q,\omega)$, which dictates the behavior of Γ for deep quenches ($\Lambda \gg \Lambda_c$), is constrained by the f-sum rule: $\int d\omega\omega\, \mathrm{Im}\chi(Q,\omega) = \pi Q^2/m$. For deep quenches—defined self-reflexively by the regime in which Γ exceeds frequencies for which $\mathrm{Im}[\chi(Q,\omega)]$ is substantially supported—our self-consistency equation reduces to $\Gamma^2(1+\Gamma^2\Delta_c^{-2}) = (8\Lambda^2 N E_R/\Delta_c)$, where $E_R = (\mathbf{k}_-^2 + \mathbf{k}_+^2/2m)$. For deep quenches, this implies a universal behavior of Γ invariant to all microscopic details of the atomic gas besides E_R.

If the cavity field and transverse drive are sufficiently nonorthogonal, $\mathbf{k}_+ \gg \mathbf{k}_-$ [15]. As a result, $\chi(\mathbf{k}_-) \gg \chi(\mathbf{k}_+)$, and the collective instability is driven by the formation of density order along $\mathbf{k}_-$ for weak quenches. Per contrast, for deep quenches, the instability arising from $\mathbf{k}_+$ dominates the one arising from $\mathbf{k}_-$. Therefore, if $\mathbf{k}_+ \gg \mathbf{k}_-$, there is a dual nature to Γ which has an inflection point at large coupling strengths, as shown in Fig. 1. By analyzing Eq. (4) close to criticality, we can extract the critical scaling exponents, classifying how the growth rate Γ depends on the deviation from the critical point $\Lambda - \Lambda_c$. For systems without zero energy excitations at finite momentum Q, $\mathrm{Im}\chi(\omega \to 0, Q) = 0$, and the rate equation can be expanded, giving $\Gamma \sim (\Lambda - \Lambda_c)^{\frac{1}{2}}$ the bosonic and attractive fermion systems, in agreement with the dissipationless Dicke model [37]. However, for systems with gapless excitations, such as free fermion systems, the expansion fails for $Q < 2k_F$, since $\mathrm{Im}\chi(\omega \to 0, Q) \sim \omega$, and the integral has finite contribution from frequencies $\omega \ll \Gamma$. In this case, $\Gamma \sim (\Lambda - \Lambda_c)$, different from the usual Dicke exponent, which characterizes bosonic and attractive fermionic systems. Notably, adding finite temperature and dissipation also modifies the Dicke scaling in physical systems, yielding $\Gamma \propto (\Lambda - \Lambda_c)$ [37], in congruence with free fermions.

Seeding the instability—Having computed the growth rate Γ, it is natural to ask, "How long does unstable growth last?" To answer this, we begin by calculating n_0 and $\rho_{Q,0}$—prefactors for the exponentially growing photon number and the density order—and compare them to estimates for n_{sat} and $\rho_{Q,\mathrm{sat}}$, where we expect nonlinear saturation effects to arise. To calculate prefactors n_0 and $\rho_{Q,0}$, we note that the instability is dominantly seeded by the density fluctuations of homogeneous atomic gas [36]. We underscore that n_0 is not a theoretical curiosity: a high-throughput experiment should be able to quantify it.

We quantify how these density fluctuations seed the instability by computing their power spectral density at the instability frequency Γ. To do so, we turn to the Laplace formalism, which allows us to propagate the linearized Heisenberg evolution arising from Eq. (1), even in the presence of an exponentially growing mode. In the Supplemental Material [36], we provide a derivation of the prefactor by leveraging the Kubo formula; we briefly sketch our general derivation here. Within the Laplace formalism, the photonic equations of motion become

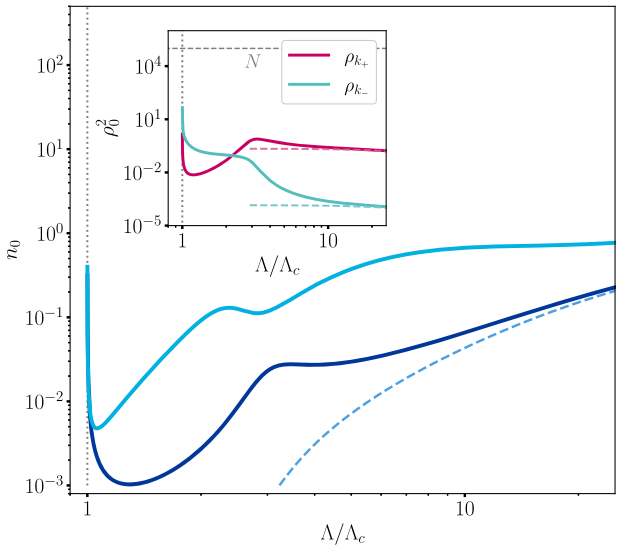

FIG. 2. Instability seeded by density fluctuations. The photon number prefactor n_0 as a function of the light-matter coupling Λ for $\Delta_c = 175E_F$ and ordering wave vectors $|\mathbf{k}_+| = 3.7k_F$, $|\mathbf{k}_-| = 0.59k_F$ for a 3D unitary Fermi gas (dark blue), corresponding to the experimental setup [15], and for $|\mathbf{k}_+| = 3.7n^{1/3}$, $|\mathbf{k}_-| = 0.59n^{1/3}$ for weakly interacting bosons with $4\pi n^{1/3}a = 1$, where a is the scattering length and n is the density. The dashed lines show the asymptotic behaviors for deep quenches. Inset: the dependence of the density ordering prefactor on Λ for the $\mathbf{k}_\pm$ modes in the same parameter regime. The gray horizontal line shows an estimate to the saturation value of density fluctuations.

$sx(s) - x(t=0) = -i\Delta_c p(s)$ and $sp(s) - p(t=0) = i\Delta_c x(s) + i\sqrt{N}\Lambda\sum_Q \rho_Q(s)$. For the atomic evolution, we use the Kubo formula, which, upon Laplace transformation, reads $\rho_Q(s) = \sqrt{N}\Lambda\chi(Q,s)x(s) + \rho_Q^0(s)$, where $\rho_Q^0(s)$ is the Laplace transform of the interaction picture evolution of $\rho_Q(t) = e^{iH_{\mathrm{at}}t}\rho_Q(t=0)e^{-iH_{\mathrm{at}}t}$. Combining the equations, we find that n_0 is given by

$$n_0 = \frac{1}{8}\left(\frac{1}{\Gamma^2} + \frac{1}{\Delta_c^2}\right)\frac{\Lambda^2\Delta_c^3}{\Lambda_c^2\sum_Q\chi(Q)} \times \sum_Q \int_0^\infty d\omega \frac{\Im\chi(Q,\omega)}{\omega^2+\Gamma^2} \Bigg/ \left(1 + \frac{\Lambda^2\Delta_c^2}{\Lambda_c^2\sum_Q\chi(Q)} \times \sum\nolimits_Q \int_{-\infty}^\infty d\omega \frac{\Im\chi(Q,\omega)\omega}{(\omega^2+\Gamma^2)^2}\right)^2, \tag{5}$$

and the density ordering prefactor $\rho_{Q,0} = (1/\sqrt{2})(\Lambda/\Lambda_c)\sqrt{[\Delta_c^3/\sum_Q\chi(Q)(\Gamma^2+\Delta_c^2)]}\chi(Q,i\Gamma)\sqrt{n_0}$. For near-critical quenches of free-fermion systems, the prefactors diverge weakly with $n_0 \sim \log(E_F/\Gamma)$ and $\rho_{Q,0} \sim \log^{1/2}(E_R/\Gamma)$, whereas for deep quenches, $n_0 = \frac{1}{8}[2 + (\Gamma^2/\Delta_c^2) + (\Delta_c^2/\Gamma^2)][\Gamma^2/(2\Gamma^2+\Delta_c^2)]^2(\Delta_c/2E_R)\sum_Q S(Q)$, $\rho_{Q,0} = (1/2\sqrt{2})(E_Q/E_R)(\Gamma^2 + \Delta_c^2/2\Delta_c^2 + \Gamma^2)$, where $S(Q)$ is the

static structure factor of the atomic gas at wave vector Q and E_Q is the recoil energy at momentum Q. The log divergence for near-critical quenches arises from the fact that the support of $\mathrm{Im}\chi(Q,\omega)$ extends to $\omega = 0$. For weakly interacting bosons or attractive fermions, the divergence near criticality becomes $n_0 \sim (1/\Gamma^2)$ and $\rho_{Q,0} \sim (1/\Gamma)$, whereas the deep quench seed expression remains the same, reflecting the f-sum rule universality.

Our asymptotics suggest the nonmonotonic behavior of n_0 and $\rho_{Q,0}$ as a function of Λ, as shown in Fig. 2. For near-critical quenches, we expect that dynamical fluctuations of the order parameter in the Ginzburg-Landau potential with a vanishing quadratic term diverge as the frequency goes to 0, implying a divergent prefactor as a function of Γ. In contrast, for deep quenches, the growth rate is so fast that the instability is sensitive only to the static fluctuations of the gas described by $S(Q)$. At the same time, the character of the unstable polaritonic mode becomes more densitylike. Thus, the prefactor—which carries a projection onto the unstable mode—picks up a factor that scales with Λ.

As the polaritonic mode grows and photons proliferate in the cavity, density modulations deplete atoms in the nodes of the waves along Q. As ρ_Q approaches $\mathcal{O}(\sqrt{N})$, nonlinearities arise to penalize further depletion of the atomic density, leading to saturation. While a more careful analysis of this saturation is required, a strict upper bound on $\rho^2_{Q,\mathrm{sat}}$ is set by N ($\sim 10^5$ in experiments), a full condensation of the density mode along Q. Juxtaposing this upper bound on $\rho^2_{Q,\mathrm{sat}}$ with $\rho^2_{Q,0}$, as plotted in the inset of Fig. 2, reveals a dynamic range of at least 5 orders of magnitude immediately away from criticality. Thus, nonlinear saturation effects are weak, and the (linear) instability should persist for multiple decades of exponential growth. The inset of Fig. 2 also reflects that $\rho_{\mathbf{k}_+,0}/\rho_{\mathbf{k}_-,0} = \chi(\mathbf{k}_+, i\Gamma)/\chi(\mathbf{k}_-, i\Gamma)$, which implies that while for shallower quenches, the prefactor for the $\mathbf{k}_-$ mode is larger than that of the $\mathbf{k}_+$ mode, the situation is reversed for deep quenches. Thus, within our saturation mechanism, for near-critical quenches, the $\mathbf{k}_-$ mode should saturate first, while for deep quenches, the $\mathbf{k}_+$ instability depletes the atoms faster.

Experimental implications—Existing experiments have been performed only in fermionic systems and typically operate in the regime where $\Delta_c/E_\mathrm{F} \sim 100$–$300$ and for quenches up to $\Lambda \sim 5\Lambda_c$ [14,15], probing primarily the region around criticality. The first condition implies that dynamics of the cavity photon are irrelevant, and the instability can be captured by studying quenches of fermions interacting all-to-all with cavity photon-mediated interactions. This, in turn, means that as a function of Λ/Λ_c, Γ does not depend on Δ_c, a fact that is captured by the negligibility of the $\Gamma^2\Delta_c^{-2}$ term in Eq. (4) in the experimental regime. The second experimental circumscription implies that the scale of the instability rate is set by E_R, highlighting the atomic character of the instability.

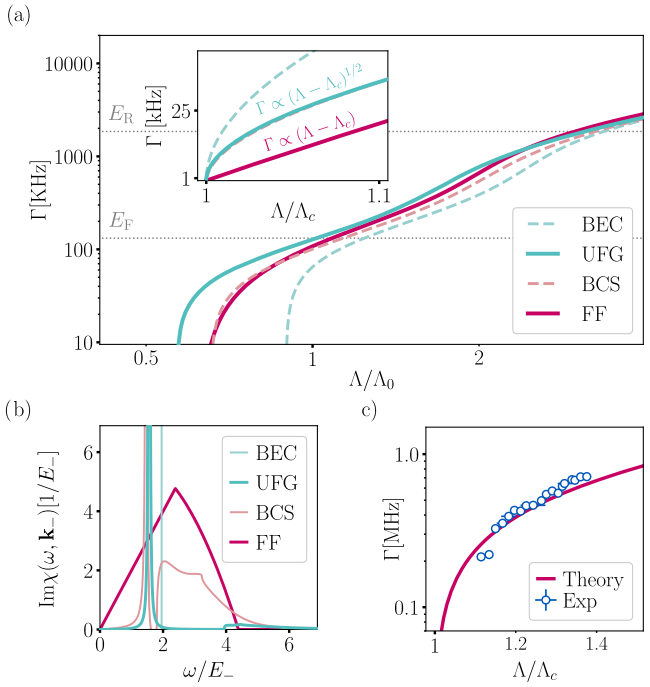

FIG. 3. Interactions and experiments. (a) Instability growth rate Γ as a function of effective coupling in 3D for different scattering lengths $1/k_\mathrm{F}a = \{-0.7, 0\}$, free fermions, and weakly interacting bosons with $4\pi n^{1/3}a = 1$. The quench strength Λ is measured in units of $\Lambda_0 = \sqrt{(\Delta_c E_\mathrm{F}/N)}[\sqrt{(\Delta_c n^{2/3}/N2m)}]$ and $\Delta_c = 100E_\mathrm{F}(100n^{2/3}/2m)$ for fermions (bosons), where m is the bosonic mass. $\mathbf{k}_+ = 3.7k_\mathrm{F}$ and $\mathbf{k}_- = 0.59k_\mathrm{F}$; $\mathbf{k}_+ = 3.7n^{1/3}$ and $\mathbf{k}_- = 0.59n^{1/3}$ for bosons. The inset indicates the scaling of the rate Γ close to criticality as a function of reduced light-matter coupling Λ/Λ_c. (b) Low-frequency behavior of $\mathrm{Im}\chi(\mathbf{k}_-,\omega)$ for free fermions, weakly interacting bosons, and across the BEC-BCS crossover within the RPA approximation. The vertical arrow indicates the delta function corresponding to the bosonic sound mode. (c) Comparison of the rate, calculated for free fermions including cavity dissipation and trap averaging, with experimental data (see Supplemental Material [36] for details) [14].

Experiments also feature finite dissipation rates arising from the leakage of photons from the cavity at a rate κ. We can capture this straightforwardly by taking $\omega \to \omega - i\kappa$ in Eq. (3) on the left-hand side but *not* on the right [36]. In Fig. 3(a), we show results comparing quenches of weakly interacting bosons (BEC) and free fermions as well as different interacting fermionic systems, including unitary Fermi gas (UFG) and superconducting state (BCS), corresponding to experiments performed on near unitary Fermi gases [15,29]. The response functions were computed using the random-phase approximation [38,39]. As shown in Fig. 3(b), distinctions between these rates arise from qualitative differences in the dynamical susceptibility of the atomic gases—compared to free fermions, interactions lead to a sharp Bogolyubov-Anderson mode at $\omega \sim c_s\mathbf{k}_-$, where c_s is the sound velocity in the atomic gas. The

differences in the Λ_c across the interacting regime arise, then, from the differences in the sound velocity across the BEC-BCS transition. In Fig. 3(c), we make an explicit comparison to experiments performed on dissipative, harmonically trapped, free fermions [14]. We find good agreement with experimental measurements upon accounting for trap induced density inhomogeneities [36].

Discussion—In our Letter, we articulate a linear stability analysis that both captures the rate at which order grows after a quench into the self-organized phase and quantifies the fluctuations that seed the instability. Our theory is quantitatively accurate in capturing existing experimental measurements of the instability rate and makes predictions for future experiments studying quenches in optical cavities where the atomic gas is strongly interacting. Moreover, the analytical tractability of the present setting in which a couple of discrete unstable collective modes arise allows us to elucidate various nontrivial aspects of many-body instabilities—e.g., the changing character of the coupled unstable modes that seed and saturate the order parameter growth. We expect that the careful, experimentally verifiable theoretical considerations of such matters in this simpler context will facilitate the analysis of more complex settings in which there are a plethora of unstable modes.

Extensions of our analysis may be useful in interpreting experiments that seek to optically control complex materials. While experiments in this burgeoning field have probed a wide variety of ordering dynamics, from charge density order [40,41] to ferroelectricity [42,43] to superconductivity [44–46], theoretical modeling of such dynamical phenomena remains limited in either microscopic detail due to their computational intractability [47–50]. Extensions of the formalism developed here could pave the way for a tractable theoretical framework for understanding how to stabilize nonthermal states of matter in solid-state settings.

Given the success of our theory in capturing experimental measurements, we conclude by highlighting a startling discrepancy between the growth rates that we uncover herein and the growth rates of short-range interacting systems where, for example in fermionic systems, E_F sets a local speed limit on the rate at which correlated order can grow [7]. For deep quenches in our setting—restricting our discussion to $\Gamma \ll \Delta_c$—Eq. (4) does not provide a bound on the rate, allowing it to *far exceed* all fermionic scales, including E_R, which quantifies the frequency at which the fastest local atomic response can occur. Fascinatingly, for deep quenches, $\Gamma \sim \sqrt{N}$.

To gain physical insight into this surprise, we can first consider why local limits arise in, e.g., short-range fermionic systems where E_F cuts off the scale of the instability rate. If the interaction is short range, the two-body relative wave function can deform to avoid the cost of the two particle interactions, a deformation that costs an energy of E_F. In contrast, the ordering dynamics of the cavity-Fermi gas system is not only *captured* by mean-field theory, it renders the (dynamical) idiosyncrasies of mean-field theory *physically manifest*: the fermions each individually react to the *collectively* determined mean field that is generated by cavity photon-mediated all-to-all interactions. The lack of a local limit on the growth rate is consistent with a panorama of theoretical findings that complicate the Lieb-Robinson phenomenology in long-range interacting systems [51]. Experiments to verify whether effects beyond our present considerations set a limit on the rate are feasible and should allow us to elucidate qualitative differences between nonequilibrium dynamics in quantum many-body systems with short- and long-range interactions.

Acknowledgments—We acknowledge stimulating interactions with H. Wu, N. Defenu, and A. Gomez-Salvador. The ETH group acknowledges funding from the Swiss National Science Foundation Project 200021_212899; the Swiss State Secretariat for Education, Research and Innovation (Contract No. UeM019-1); and NCCR SPIN. E. D. acknowledges funding from ARO Grant No. W911NF-21-1-0184. S. C. is grateful for support from the NSF under Grant No. DGE-1845298 and for the hospitality of the Institute of Theoretical Physics at ETH, Zürich. J. P. B. and T. Z. acknowledge funding from the Swiss State Secretariat for Education, Research and Innovation (Grants No. MB22.00063 and No. UeM019-5.1). T. G. and C.-M. H. acknowledge support by the Swiss National Science Foundation under Division II Grants No. 200020-188687 and No. 200020-219400 and would like to thank the Institut Henri Poincaré (UAR 839 CNRS-Sorbonne Université) and the LabEx CARMIN (ANR-10-LABX-59-01) for their support. C.-M. H. acknowledges support in part by Grant No. NSF PHY-1748958 to the Kavli Institute for Theoretical Physics (KITP). S. B. J. acknowledges support from the Deutsche Forschungsgemeinschaft (DFG): Projects A4 and A5 in SFB/Transregio 185: "OSCAR."

[1] T. W. B. Kibble, Topology of cosmic domains and strings, J. Phys. A **9**, 1387 (1976).
[2] I. Chuang, R. Durrer, N. Turok, and B. Yurke, Cosmology in the laboratory: Defect dynamics in liquid crystals, Science **251**, 1336 (1991).
[3] W. H. Zurek, Cosmological experiments in superfluid helium, Nature (London) **317**, 505 (1985).
[4] L. E. Sadler, J. M. Higbie, S. R. Leslie, M. Vengalattore, and D. M. Stamper-Kurn, Spontaneous symmetry breaking in a quenched ferromagnetic spinor Bose–Einstein condensate, Nature (London) **443**, 312 (2006).
[5] G.-B. Jo, Y.-R. Lee, J.-H. Choi, C. A. Christensen, T. H. Kim, J. H. Thywissen, D. E. Pritchard, and W. Ketterle, Itinerant ferromagnetism in a Fermi gas of ultracold atoms, Science **325**, 1521 (2009).
[6] C. Sanner, E. J. Su, W. Huang, A. Keshet, J. Gillen, and W. Ketterle, Correlations and pair formation in a repulsively interacting Fermi gas, Phys. Rev. Lett. **108**, 240404 (2012).

[7] D. Pekker, M. Babadi, R. Sensarma, N. Zinner, L. Pollet, M. W. Zwierlein, and E. Demler, Competition between pairing and ferromagnetic instabilities in ultracold Fermi gases near Feshbach resonances, Phys. Rev. Lett. **106**, 050402 (2011).
[8] L. E. Sadler, J. M. Higbie, S. R. Leslie, M. Vengalattore, and D. M. Stamper-Kurn, Spontaneous symmetry breaking in a quenched ferromagnetic spinor Bose–Einstein condensate, Nature (London) **443**, 312 (2006).
[9] M. Vengalattore, S. R. Leslie, J. Guzman, and D. M. Stamper-Kurn, Spontaneously modulated spin textures in a dipolar spinor Bose-Einstein condensate, Phys. Rev. Lett. **100**, 170403 (2008).
[10] K. E. Strecker, G. B. Partridge, A. G. Truscott, and R. G. Hulet, Formation and propagation of matter-wave soliton trains, Nature (London) **417**, 150 (2002).
[11] J. H. V. Nguyen, P. Dyke, D. Luo, B. A. Malomed, and R. G. Hulet, Collisions of matter-wave solitons, Nat. Phys. **10**, 918 (2014).
[12] G. Lamporesi, S. Donadello, S. Serafini, F. Dalfovo, and G. Ferrari, Spontaneous creation of Kibble–Zurek solitons in a Bose–Einstein condensate, Nat. Phys. **9**, 656 (2013).
[13] N. Navon, A. L. Gaunt, R. P. Smith, and Z. Hadzibabic, Critical dynamics of spontaneous symmetry breaking in a homogeneous Bose gas, Science **347**, 167 (2015).
[14] Z. Wu, J. Fan, X. Zhang, J. Qi, and H. Wu, Signatures of prethermalization in a quenched cavity-mediated long-range interacting Fermi gas, Phys. Rev. Lett. **131**, 243401 (2023).
[15] T. Zwettler, G. del Pace, F. Marijanovic, S. Chattopadhyay, T. Bühler, C.-M. Halati, L. Skolc, L. Tolle, V. Helson, G. Bolognini, A. Fabre, S. Uchino, T. Giamarchi, E. Demler, and J.-P. Brantut, Non-equilibrium dynamics of long-range interacting fermions, arXiv:2405.18204.
[16] J. Larson, G. Morigi, and M. Lewenstein, Cold Fermi atomic gases in a pumped optical resonator, Phys. Rev. A **78**, 023815 (2008).
[17] Q. Sun, X.-H. Hu, A.-C. Ji, and W. M. Liu, Dynamics of a degenerate Fermi gas in a one-dimensional optical lattice coupled to a cavity, Phys. Rev. A **83**, 043606 (2011).
[18] X. Guo, Z. Ren, G. Guo, and J. Peng, Ultracold Fermi gas in a single-mode cavity: Cavity-mediated interaction and BCS-BEC evolution, Phys. Rev. A **86**, 053605 (2012).
[19] F. Piazza and P. Strack, Quantum kinetics of ultracold fermions coupled to an optical resonator, Phys. Rev. A **90**, 043823 (2014).
[20] F. Piazza and P. Strack, Umklapp superradiance with a collisionless quantum degenerate Fermi gas, Phys. Rev. Lett. **112**, 143003 (2014).
[21] Y. Chen, H. Zhai, and Z. Yu, Superradiant phase transition of Fermi gases in a cavity across a Feshbach resonance, Phys. Rev. A **91**, 021602 (2015).
[22] E. Colella, R. Citro, M. Barsanti, D. Rossini, and M.-L. Chiofalo, Quantum phases of spinful Fermi gases in optical cavities, Phys. Rev. B **97**, 134502 (2018).
[23] P. Domokos and H. Ritsch, Collective cooling and self-organization of atoms in a cavity, Phys. Rev. Lett. **89**, 253003 (2002).
[24] C. Maschler and H. Ritsch, Ultracold atoms in optical lattices generated by quantized light field, Eur. Phys. J. D **46**, 545 (2008).
[25] D. Nagy, G. Kónya, G. Szirmai, and P. Domokos, Dicke-model phase transition in the quantum motion of a Bose-Einstein condensate in an optical cavity, Phys. Rev. Lett. **104**, 130401 (2010).
[26] A. T. Black, H. W. Chan, and V. Vuletić, Observation of collective friction forces due to spatial self-organization of atoms: From Rayleigh to Bragg scattering, Phys. Rev. Lett. **91**, 203001 (2003).
[27] K. Baumann, C. Guerlin, F. Brennecke, and T. Esslinger, Dicke quantum phase transition with a superfluid gas in an optical cavity, Nature (London) **464**, 1301 (2010).
[28] X. Zhang, Y. Chen, Z. Wu, J. Wang, J. Fan, S. Deng, and H. Wu, Observation of a superradiant quantum phase transition in an intracavity degenerate Fermi gas, Science **373**, 1359 (2021).
[29] V. Helson, T. Zwettler, F. Mivehvar, E. Colella, K. Roux, H. Konishi, H. Ritsch, and J.-P. Brantut, Density-wave ordering in a unitary Fermi gas with photon-mediated interactions, Nature (London) **618**, 716 (2023).
[30] H. Ritsch, P. Domokos, F. Brennecke, and T. Esslinger, Cold atoms in cavity-generated dynamical optical potentials, Rev. Mod. Phys. **85**, 553 (2013).
[31] Y. Chen, Z. Yu, and H. Zhai, Superradiance of degenerate Fermi gases in a cavity, Phys. Rev. Lett. **112**, 143004 (2014).
[32] J. Keeling, M. J. Bhaseen, and B. D. Simons, Fermionic superradiance in a transversely pumped optical cavity, Phys. Rev. Lett. **112**, 143002 (2014).
[33] T. D. Farokh Mivehvar, Francesco Piazza, and H. Ritsch, Cavity QED with quantum gases: New paradigms in many-body physics, Adv. Phys. **70**, 1 (2021).
[34] For example, the experimental setup in Ref. [15] involves multiple polarizations used to offset the optical lattice arising from a pump induced AC stark field. These polarizations play a trivial role in the superradiant physics, merely modifying the effective light-matter coupling [15].
[35] The doubling of the photon growth rate compared to the rate of density order formation is due to the fact that $\rho_q \propto \alpha$, the coherence of the photon, while $n \propto \alpha^2$.
[36] See Supplemental Material at http://link.aps.org/supplemental/10.1103/w2vx-t1mr for details.
[37] M. J. Bhaseen, J. Mayoh, B. D. Simons, and J. Keeling, Dynamics of nonequilibrium Dicke models, Phys. Rev. A **85**, 013817 (2012).
[38] N. Dupuis, *Field Theory of Condensed Matter And Ultracold Gases* (World Scientific Publishing Europe Limited, Singapore, 2023), Vol. 1.
[39] L. He, Dynamic density and spin responses of a superfluid Fermi gas in the BCS–BEC crossover: Path integral formulation and pair fluctuation theory, Ann. Phys. (Amsterdam) **373**, 470 (2016).
[40] A. Zong, P. E. Dolgirev, A. Kogar, Y. Su, X. Shen, J. A. W. Straquadine, X. Wang, D. Luo, M. E. Kozina, A. H. Reid, R. Li, J. Yang, S. P. Weathersby, S. Park, E. J. Sie, P. Jarillo-Herrero, I. R. Fisher, X. Wang, E. Demler, and N. Gedik, Role of equilibrium fluctuations in light-induced order, Phys. Rev. Lett. **127**, 227401 (2021).
[41] A. Kogar *et al.*, Light-induced charge density wave in $LaTe_3$, Nat. Phys. **16**, 159 (2020).

[42] X. Li, T. Qiu, J. Zhang, E. Baldini, J. Lu, A. M. Rappe, and K. A. Nelson, Terahertz field–induced ferroelectricity in quantum paraelectric $SrTiO_3$, Science **364**, 1079 (2019).

[43] T. F. Nova, A. S. Disa, M. Fechner, and A. Cavalleri, Metastable ferroelectricity in optically strained $SrTiO_3$, Science **364**, 1075 (2019).

[44] M. Mitrano, A. Cantaluppi, D. Nicoletti, S. Kaiser, A. Perucchi, S. Lupi, P. Di Pietro, D. Pontiroli, M. Riccò, S. R. Clark, D. Jaksch, and A. Cavalleri, Possible light-induced superconductivity in K_3C_{60} at high temperature, Nature (London) **530**, 461 (2016).

[45] M. Budden, T. Gebert, M. Buzzi, G. Jotzu, E. Wang, T. Matsuyama, G. Meier, Y. Laplace, D. Pontiroli, M. Riccò, F. Schlawin, D. Jaksch, and A. Cavalleri, Evidence for metastable photo-induced superconductivity in K_3C_{60}, Nat. Phys. **17**, 611 (2021).

[46] E. Rowe, B. Yuan, M. Buzzi, G. Jotzu, Y. Zhu, M. Fechner, M. Först, B. Liu, D. Pontiroli, M. Riccò, and A. Cavalleri, Resonant enhancement for photo-induced superconductivity in K_3C_{60}, Nat. Phys. **19**, 1821 (2023).

[47] J. Bauer, M. Babadi, and E. Demler, Dynamical instabilities and transient short-range order in the fermionic Hubbard model, Phys. Rev. B **92**, 024305 (2015).

[48] P. E. Dolgirev, M. H. Michael, A. Zong, N. Gedik, and E. Demler, Self-similar dynamics of order parameter fluctuations in pump-probe experiments, Phys. Rev. B **101**, 174306 (2020).

[49] C. Stahl and M. Eckstein, Electronic and fluctuation dynamics following a quench to the superconducting phase, Phys. Rev. B **103**, 035116 (2021).

[50] A. Picano and M. Eckstein, Accelerated gap collapse in a Slater antiferromagnet, Phys. Rev. B **103**, 165118 (2021).

[51] N. Defenu, T. Donner, T. Macrì, G. Pagano, S. Ruffo, and A. Trombettoni, Long-range interacting quantum systems, Rev. Mod. Phys. **95**, 035002 (2023).